Classical 1,2,4-Triboracyclopentanes and Their Rearrangement into Nonclassical 2-Boryl-1,3-diboracyclobutanes: Intramolecular C–H Bond Activation by a B–B Moiety

David Scheschkewitz,[a] Peter Amseis,[a] Gertraud Geiseler,[a] Werner Massa,[a]
Matthias Hofmann,[b] and Armin Berndt*[a]

Keywords: Ab initio computations / Boron heterocycles / Three-centre, two-electron bonds

1,2,4-Triboracyclopentanes **1a**–**c** in solution spontaneously transform into their nonclassical isomers **2a**–**c**. These have been characterised by NMR spectroscopy and X-ray structural analyses. Compounds **2a**–**c** are strongly distorted when compared with the five-membered ring of **1a**, the structure of which was determined for comparison. In addition, the pattern of the substituents at the boron centres in **2a**,**b** is different from that in **1a**,**b**. This can be rationalised on the basis of a rapid topomerisation in **2c** as determined by analysis of its temperature dependent ^{13}C NMR spectra. The environment of the boron centres B1 and B3 is exchanged by transforming the two 3c–2e bonds which both involve B1 into a B2–H and a B1–C 2c–2e bond. This leads to the 2-boryl-1,3-diboracyclobutane **4c** and formation of corresponding new 3c–2e bonds employing B3 gives the topomer of **2c**. The low barrier of this topomerisation reveals that **2a**–**c** may also be regarded as nonclassical isomers of the 2-boryl-1,3-diboracyclobutanes **4a**–**c**. Ab initio computations of models at the MP4SDTQ/6-311+G**// MP2/6-311+G** levels support this interpretation. In addition, they show that the transformation of **1u** to **2u** occurs by an intramolecular C–H bond activation process initiated by the B–B moiety. Derivatives of the type **1** and **2** described here represent the first examples of 1,2-diboron heterocycles which can be isolated as classical as well as nonclassical isomers.

Introduction

Classical forms of unsubstituted 1,2-diboron heterocycles of type **I–III** (Scheme 1) have been computed to be considerably higher in energy than their nonclassical forms **IV–VI**.[1,2] This is due to the two-electron aromaticity of **IV** and homoaromaticity of **V** and **VI**, respectively. The electron deficiency at the boron atoms in **I–III** is reduced in **IV–VI** by formation of two three-centre, two-electron (3c–2e) bonds. Experimentally, derivatives are known for nonclassical **IV**[3] and **V**[2] as well as for classical **II**[4] and **III**.[5] While the boron atoms of all nonclassical species bear only weakly donating substituents, those of the experimentally known classical ones carry amino substituents which strongly reduce the electron deficiency at these boron atoms. As a consequence, isomerisation of the classical compounds **II** or **III** into nonclassical compounds of type **V** or **VI** has not been observed so far. Recently, 1,2,4-triboracyclopentanes with only weakly donating substituents at the boron atoms became accessible in their classical form **1**.[6]

In this paper we show that 1,2,4-triboracyclopentanes **1a**–**c** (Scheme 2) isomerise into nonclassical isomers **2a**–**c**. Ab initio computations at the MP2/6-311+G** level[7] for the prototypes **1u** and **2u** (Scheme 3) reveal that these transformations are intramolecular C–H bond activations by B–B moieties. However, **2a**,**b** are isomers of the products to be expected from these C–H bond activations in **1a**,**b**. This discrepancy can be rationalised by an additional rearrangement via **4a**,**b** (Scheme 4) which shows up in **2c** as a topomerisation via **4c**. Therefore, compounds of type **2** may be regarded equally well as nonclassical 1,2,4-triboracyclopentanes and as nonclassical 2-boryl-1,3-diboracyclobutanes.

Results and Discussion

Syntheses and NMR Characterisation

Details of the preparation of 1,2,4-triboracyclopentanes **1a**,**b**[6] and **1d**[6] are described in the experimental section. Compound **1d** does not react with duryllithium to yield **1c** which, finally, was synthesised by oxidation of its dianion $1c^{2-}$. This can be obtained by addition of duryllithium to the borenate **3**.[6] In $CDCl_3$ solution, **1a**,**b** transform into their nonclassical isomers **2a**,**b** within four and nine days, respectively. Isomerisation of **1c** into **2c** requires only 2 h in diethyl ether. Interestingly, $CDCl_3$ solutions of the stereo-

---

[a] Fachbereich Chemie der Universität Marburg,
Hans-Meerwein-Strasse, 35032 Marburg
Fax: +49-6421-2828917
E-mail: berndt@chemie.uni-marburg.de
[b] Anorganisch-Chemisches Institut der Universität Heidelberg,
Im Neuenheimer Feld 270, 69120 Heidelberg

DOI: 10.1002/ejic.200500279

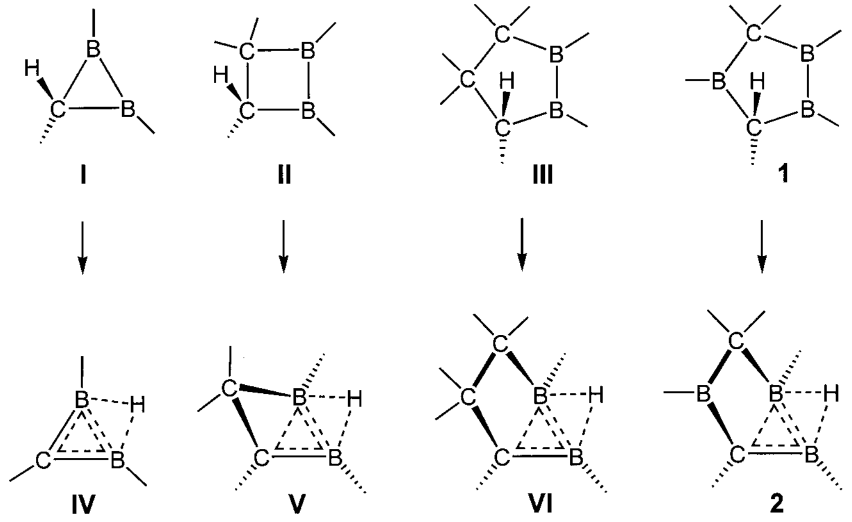

Scheme 1.

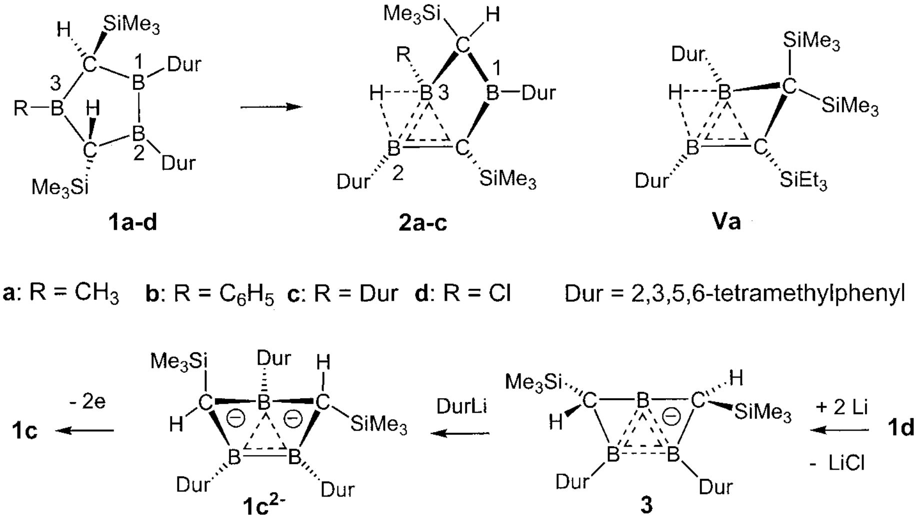

Scheme 2.

isomers of **1a**,**b** having the trimethylsilyl substituents in *cis* positions[8] do not show any isomerisation over a period of three months.

Compounds **2a–c** were characterised by ^{1}H, ^{13}C and ^{11}B NMR spectroscopy. The chemical shifts of the skeleton atoms of **2a**,**b** are in good agreement with those computed for **2u** at the IGLO/II/MP2/6-31+G* level and resemble those of **Va** (see Table 1).

Table 1. Selected NMR chemical shifts [ppm] of **2a**–**c**, **Va** (exp.) and **2u** (calcd. at IGLO/II/MP2/6-31+G*).

	2a	2b	2c	2u	Va
δ^{11}B B3[a]	0	–2	ca. 30[b]	–6.0	3[c]
δ^{11}B B2[a]	48	42	ca. 47[b]	46.9	
δ^{11}B B1[a]	56	57	ca. 47[b]	48.5	48[d]
δ^{13}C C1[a]	74.6	70.7	105	72.6	68.2[e]
δ^{13}C C2[a]	27.6	26.8	24.8	16.6	32.1[f]

[a] Numbering as in Figures 1, 2, 3 and 4. [b] Broad signal. [c] B1. [d] B2. [e] C3. [f] C4.

These chemical shifts are characteristic for homoaromatic species containing a 3c–2e bond between one carbon and two boron atoms. Compounds **2a–c** are rare examples of homoaromatics having two-membered homobridges. The boron centres B1 of **2a**,**b**, which are not part of the 3c–2e bond, are considerably shielded (48, 42 ppm) compared with those of **1a**,**b** (88, 82 ppm). This can be explained mainly by the interactions of the formally empty p orbital at B1 with the 3c–2e bond between B2, B3 and C1 (see NBO analysis of **2u** in section "Ab initio computations").

The substitution patterns at the boron atoms of **2a**,**b** are different from those of the precursors **1a**,**b**. While the boron centres between two carbon atoms carry a methyl or phenyl group in **1a**,**b**, it is a duryl group in **2a**,**b**. The methyl and phenyl substituents are found at a boron atom *adjacent* to a boron atom in **2a**,**b**. This was demonstated for **2a**,**b** by the X-ray structure analyses discussed below and for **2a** in solution by a selectively ^{11}B-decoupled ^{13}C NMR spectrum.

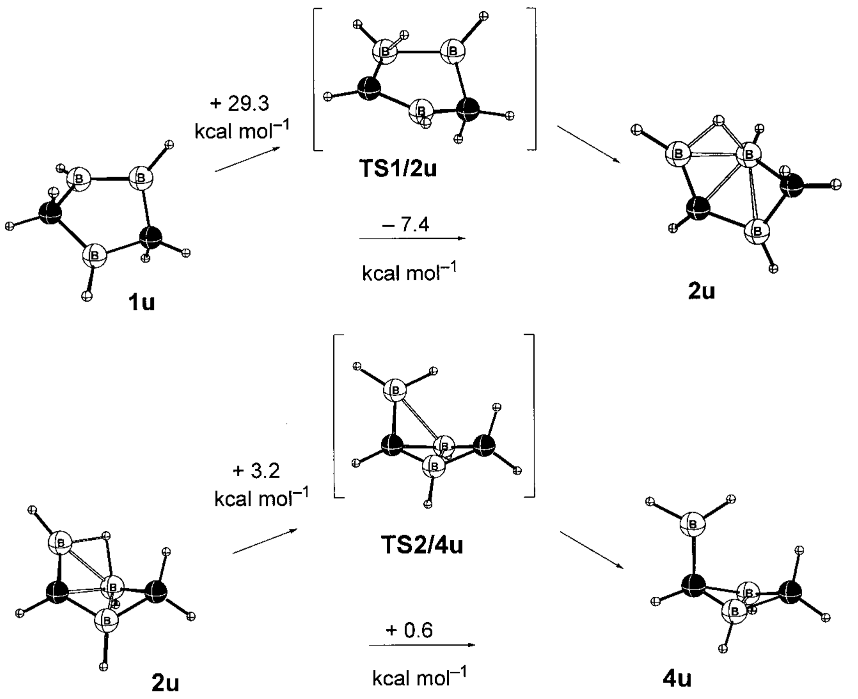

Scheme 3.

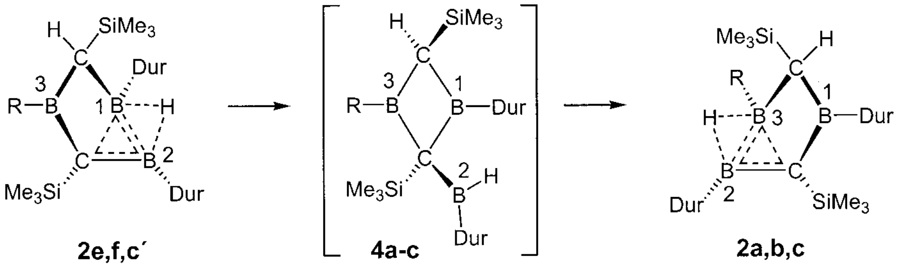

a,e: R = CH_3 **b,f**: R = C_6H_5 **c,c′**: R = Dur

Scheme 4.

Decoupling using the frequency corresponding to the chemical shift $\delta^{11}B$ = –2 ppm strongly sharpens the ^{13}C NMR signal of the boron bound methyl group at 4.9 ppm. This indicates this methyl group to be bound to the pentacoordinate boron atom. Computations for **2u** (see below) clearly support the assignment of the most shielded boron atom to that of the highest coordination number.

The chemical shifts of the skeleton atoms of **2c** are distinctly different from those of **2a**,**b**. There is no sharp ^{11}B signal at about δ = 0 for a pentacoordinate boron atom but only a broad shoulder at about 30 ppm of a very broad signal at about 47 ppm. The ^{13}C NMR spectrum of **2c** at ambient temperature shows signals for only two different kinds of duryl substituents and not for three as would be expected from its asymmetric structure which has been unambiguously deduced from the X-ray analysis described below. However, at –90 °C signals for three different duryl substituents can be observed which broaden at higher temperatures and show coalescence between –70 and –60 °C, respectively. From the chemical shift differences $\delta\nu$ of corresponding signals and their coalescence temperatures T_c, the following $\Delta G^{\#}$ values can be calculated using Equation (1): 9.2, 10.0, 9.7 and 10.0 kcal mol⁻¹.

$$\Delta G^{\#} = 4.57 \cdot T_c \cdot [9.97 + \log (T_c/\delta\nu)] \qquad (1)$$

On average, a barrier of exchange of 9.7 kcal mol⁻¹ can be obtained. We have assigned this barrier to the enantiomerisation of **2c′** to **2c** which arises through opening of the 3c–2e bonds in **2c′** to form the 2-boryl-1,3-diboracyclobutane **4c** and the corresponding new 3c–2e bonds employing the C1–B3 and B2–H bond. These transformations lead to **2c**, the enantiomer of planar-chiral **2c′**. The enantiomerisation of **2c** can be observed by NMR spectroscopy because it includes a topomerisation of two duryl substituents.

On the basis of the topomerisation of **2c′**, the unexpected pattern of substituents in **2a**,**b** can easily be explained by the corresponding process leading to isomerisation instead of topomerisation. Opening of both 3c–2e bonds in the primarily formed **2e**,**f** generates the classical 2-boryl-1,3-diboretanes **4a**,**b.** If the ring boron centre carrying the sterically less demanding substituent is employed in reforming the corresponding 3c–2e bonds, **2a**,**b** are obtained which are isomers of **2e**,**f**.

Crystal Structures

Figures 1, 2, 3 and 4 show the structures of **1a** and **2a–c** in the crystal. Characteristic distances and angles of **2a–c** and **1a** are compared with those computed for **2u** (Table 2).

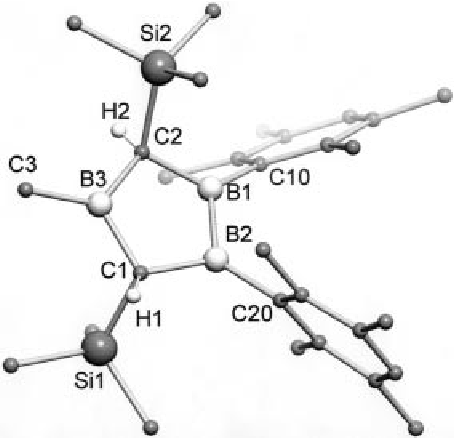

Figure 1. Structure of **1a** in the crystal. Most of the hydrogen atoms have been omitted for clarity. Selected bond lengths [pm] and angles [°] (completing Table 2): C1–B3 156.6(3), B3–C2 157.5(3), C2–B1 156.0(2), C1–Si1 189.8(2), B1–C10 158.0(2), C2–Si2 191.6(2), B2–C20 157.6(2); B1–C2–B3 107.6(1).

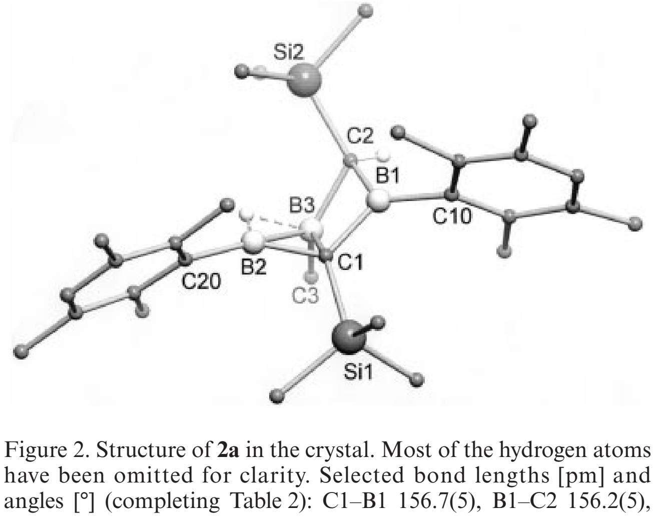

Figure 2. Structure of **2a** in the crystal. Most of the hydrogen atoms have been omitted for clarity. Selected bond lengths [pm] and angles [°] (completing Table 2): C1–B1 156.7(5), B1–C2 156.2(5), C2–B3 160.8(5), C1–Si1 188.3(3), B1–C10 159.0(5), C2–Si2 185.8(4), B3–C3 158.1(5), B2–C20 155.6(5); C1–B1–C2 106.6(3), B1–C2–B3 78.2(3).

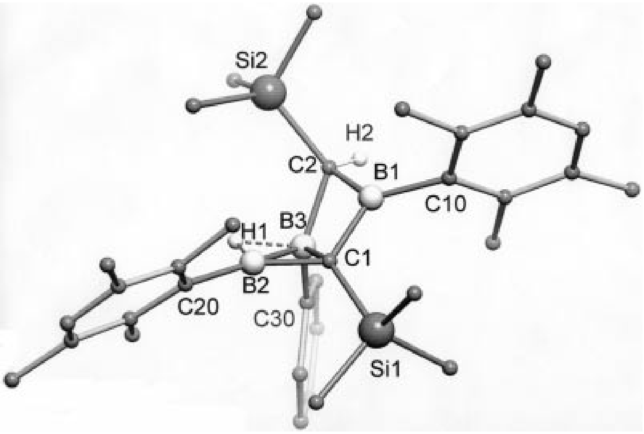

Figure 3. Structure of **2b** in the crystal. Most of the hydrogen atoms have been omitted for clarity. Selected bond lengths [pm] and angles [°] (completing Table 2): C1–B1 156.9(3), B1–C2 155.8(3), C2–B3 160.8(3), C1–Si1 189.3(2), B1–C10 157.9(3), C2–Si2 185.8(2), B3–C30 158.1(3), B2–C20 155.3(3); C1–B1–C2 107.9(2), B1–C2–B3 76.8(1).

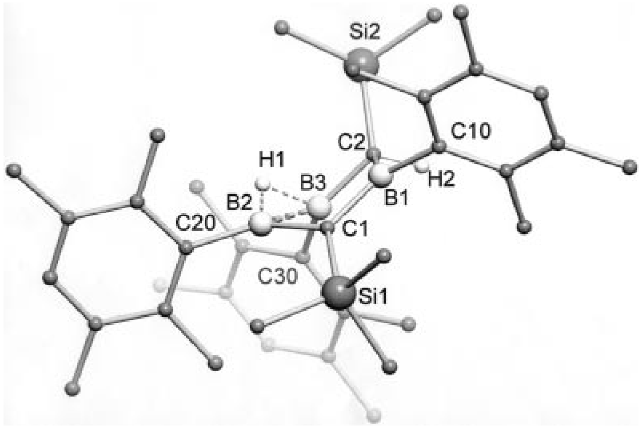

Figure 4. Structure of one of the two independent molecules **2c** in the crystal structure of **2c**·pentane. Most of the hydrogen atoms have been omitted for clarity. Selected bond lengths [pm] and angles [°] (completing Table 2): C1–B1 151.8(8), B1–C2 160.5(8), C2–B3 153.3(8), C1–Si1 189.2(6), B1–C10 159.3(7), C2–Si2 186.9(6), B3–C30 156.6(8), B2–C20 155.5(7); C1–B1–C2 109.7(4), B1–C2–B3 92.7(4).

The five-membered rings of **2a–c** are strongly distorted in comparison with that in **1a**. This can be demonstrated, inter alia, by the much shorter transannular C1···B3 distances in **2a–c** [178.0(5), 179.6(3) and 219.9(7) pm, respectively] compared with the shortest in **1a** [C2···B2 = 261.6(3) pm]. The bonding distances and angles of the C1B2B3 moiety of **2a**,**b** resemble those of the corresponding part of homoaromatic **Va**[3] (Table 2). Elongation of C1···B3 in **2a**,**b** relative to **Va** can be explained by weakening of the 3c–2e bond due to interaction with the formally empty orbital at B1 (see computations). For **2c**, the transannular B···C distance (219.9 pm) is about midway between those of **2a**,**b** and **1a**. In **2a** the C1,B1,B3 plane is folded towards the C1,B2,B3 and B1,C2,B3 planes by angles of 48 and 25°, respectively. In **2c** the corresponding angles are only 39 and 6°. Clearly, the sterically demanding duryl substituent at B3 in **2c** prevents the strong folding present in **2a,b** and **2u**, all of which lack a large substituent at the boron centre B3.

Table 2. Comparison of characteristic distances [pm] and angles [°] of **2a**–**c**, **Va**, **1a** (exp.) and **2u** (calcd. at MP2/6-311+G**).

	2u	**2a**	**2b**	**2c**·pentane	**Va**	**1a**
B2–B3	180.3	186.9(6)	187.2(3)	192.4(9)	179.9(3)[a]	175.9(2)[b]
C1–B2	147.1	149.5(5)	147.8(3)	146.5(7)	147.2(3)[c]	156.0(2)
C1···B3	180.5	178.0(5)	179.6(3)	219.9(9)	172.3(3)[d]	263.2(2)[e]
B1···B3	193.1	200.0(5)	196.8(3)	227.3(8)	–	252.9(3)[f]
C1–B2–B3	66.0	62.7(2)	63.6(1)	79.7(4)	62.7(1)[g]	104.8(1)[h]
B2–C1–B3	65.9	69.0(2)	69.0(1)	59.4(4)	68.0(1)[i]	106.6(1)
C1–B3–B2	48.1	48.3(2)	47.5(1)	41.0(3)	49.3(1)[j]	111.9(1)[k]
B2–B3–C1–B1	–145.3	–131.9(3)	–133.6(2)	–140.7(5)	133.7(2)[l]	158.6(2)[m] 163.5(2)[n]

[a] B2–B1. [b] B1–B2. [c] C3–B2. [d] C3···B1. [e] C1···B1. [f] B3···B2. [g] B1–B2–C3. [h] B1–B2–C1. [i] B2–C3–B1. [j] C3–B1–B2. [k] C1–B3–C2. [l] B2–B1–C3–C4, positive sign since the corresponding enantiomer was used. [m] B2–B1–C1–B3. [n] B1–B2–C2–B3.

Ab Initio Computations

Energies and geometries of model compounds **1u** and **2u** were computed at the MP2/6-311+G** level.[7] Bond lengths and angles obtained for **2u** are in good agreement (Table 2) with the corresponding data from the X-ray crystal structure determinations of **2a**,**b**. Chemical shifts computed at the IGLO/II/MP2/6-31+G* level for **2u** agree (Table 1) with the experimental data of **2a**,**b** but not with those of **2c**. This indicates the structure of **2c** to be different from those of **2a**,**b** in solution as well.

NBO analyses for **2u** reveal a 3c–2e bond between the neighbouring boron atoms and the formally tricoordinate carbon atom occupied by 1.84 electrons. The 0.26 electrons in the p orbital of the boron centre between carbon atoms indicate its interaction with the CB_2 3c–2e bond and explain the NMR shielding of the boron atom of the two-membered homo bridge. This interaction is essential for the stabilisation of **2u** relative to **1u** by 7.4 kcal mol^{-1}: the related nonclassical **VIu** with CH_2 instead of BH in the two-membered homo bridge is only 0.5 kcal mol^{-1} lower in energy than the classical C_s symmetric **IIIu**.[2,9]

The transition state **TS1/2u** for the transformation of **1u** into **2u** was computed to be 29.3 kcal mol^{-1} higher in energy than **1u**. **TS1/2u** has a short C–B distance (151.8 pm), a very long C–H (159.9 pm) distance as well as short (130.9 pm) and long (158.1 pm) B–H distances. According to an NBO analysis it contains a 3c–2e C–H–B bridge occupied by 1.79 electrons (29% at C, 24% at B and 37% at H). Only 4 and 7% of the two electrons are found in the p orbitals of the adjacent boron centres. This transition state thus describes the activation of a C–H bond by a neighbouring B–B moiety. The five-membered ring of the transition state is still considerably less distorted than that of the product **2u**.

Computations also revealed that classical **4u** is only 0.6 kcal mol^{-1} higher in energy than nonclassical **2u** and that the barrier for the **2u** → **4u** rearrangement via transition state **TS2/4u** is only 3.2 kcal mol^{-1}.

Compound **4u** is considerably stabilised by C–B hyperconjugation as revealed by an NBO analysis which showed the formally empty orbitals of the boron atoms to be occupied by 0.145 and 0.163 electrons at the boryl and ring boron centres, respectively. This stabilisation is certainly reduced by the substituents in **4a–c** and, as a result, the barrier from **2e**,**f**,**c′** to **2a**,**b**,**c** can be expected to be larger.

Conclusions

Classical and nonclassical 1,2,4-triboracyclopentanes **1a–c** and **2a–c** are the first representatives of 1,2-diboron heterocycles which can be isolated as classical as well as nonclassical isomers. Isomerisation of **1a**,**b** can be easily observed and computations for models reveal an intramolecular C–H bond activation by a B–B moiety as the mechanism for this process. Nonclassical 1,2,4-triboracyclopentanes **2a–c** are only slightly lower in energy than the corresponding classical 2-boryl-1,3-diboretanes **4a–c** which are considerably stabilised by C–B hyperconjugation, the general alternative to stabilisation by formation of 3c–2e bonds. Compounds of type **2** may therefore be regarded as nonclassical 2-boryl-1,3-diboracyclobutanes as well as nonclassical 1,2,4-triboracyclopentanes.

Experimental Section

General: Reactions were carried out under dry argon or nitrogen using standard Schlenk techniques. Solvents were dried, distilled and saturated with nitrogen. Glassware was dried with a heat gun under high vacuum. ^{1}H, ^{13}C NMR spectroscopy: Bruker DRX 200 and Bruker AC 500 instruments, ^{11}B NMR: Bruker DRX 200 instrument. The NMR references used were Me_4Si and $BF_3{\cdot}Et_2O$. Melting points (uncorrected) were measured under argon.

4-Methyl-1,2-bis(2′,3′,5′,6′-tetramethylphenyl)-*trans*-3,5-bis(trimethylsilyl)-1,2,4-triboracyclopentane (1a): MeLi solution (Et_2O, 1.6 M, 4.20 mL) was added by syringe to a solution of **1d** (3.45 g, 6.8 mmol) in Et_2O (50 mL) at –78 °C. The solution was then allowed to reach –10 °C over 1 h with stirring. Stirring was then suspended to allow the salts to settle and the solution was decanted through a precooled reversed frit (–15 °C, about 4 cm diameter). All solvents were removed at –10 °C. The yellow residue consisted of spectroscopically pure **1a** which was used for subsequent reactions immediately after preparation. Yield: 3.31 g (99%) of deeply yellow **1a**, m.p. 105–106 °C (dec.) ^{1}H NMR (300 MHz, $CDCl_3$, 25 °C): δ = 6.88 (s, 2 H, Dur-H), 3.31 (s, 2 H, BCH), 2.12–1.98 (br., 24 H in total), 1.10 (s, 3 H, BCH_3), 0.03 (s, 18 H, $SiMe_3$) ppm. $^{13}C\{^{11}B\}$NMR (125 MHz, $CDCl_3$, –10 °C): δ = 149.2 (s, *i*-C), 132.8, 131.5 (both s, *o*- and *m*-C), 130.0 (d, *p*-C), 66.4 [d, ^{1}J(C,H)

= 107 Hz, BCH], 20.5, 19.5 (both q, Dur-CH_3), 13.9 [br. q, ^1J(C,H) = 120 Hz, BCH_3], 2.8 (q, $SiMe_3$) ppm. ^{11}B NMR (96 MHz, $CDCl_3$, 25 °C): δ = 104 (2B), 88 (1B) ppm.

4-Phenyl-1,2-bis(2′,3′,5′,6′-tetramethylphenyl)-*trans*-3,5-bis(trimethylsilyl)-1,2,4-triboracyclopentane (1b): PhLi solution (cyclohexane/Et_2O, 1.85 M, 2.05 mL) was added to a solution of **1d** (1.91 g, 3.8 mmol) in Et_2O (50 mL) at –78 °C. The mixture was allowed to reach room temperature over 2 h and stirring was continued for 1 h at this temperature. The solvents were removed in vacuo and the residue was digested with pentane (50 mL). The salts were separated from the deep yellow solution by filtration with a reversed frit and washed with pentane (10 mL). The filtrates were reduced to dryness in vacuo yielding spectroscopically pure **1b**. Yield: 2.04 g (99%) of deep yellow **1b**, m.p. 99 °C (dec.). For spectroscopic data see ref.[6]

4-Chloro-1,2-bis(2′,3′,5′,6′-tetramethylphenyl)-*trans*-3,5-bis(trimethylsilyl)-1,2,4-triboracyclopentane (1d): $B(OMe)_3$ (9.15 g, 88.0 mmol, 10 mL) was added slowly by syringe to a suspension of dilithium-2,3-bis(2′,3′,5′,6′-tetramethylphenyl)-1,4-bis(trimethylsilyl)-2,3-diboratabuta-1,3-diene[6] (13.4 g, 21.5 mmol) in pentane (200 mL) at –78 °C. The mixture was allowed to reach room temperature during which time it gradually became yellow. Stirring was continued overnight and the solvents were then removed in vacuo. The viscous residue was thoroughly dried in vacuo for 2 h and was then digested with pentane (200 mL) and cooled again to –78 °C. After addition of BCl_3 (30 g, 256 mmol) with a syringe, the mixture was warmed to room temperature over 2 h and stirring was continued for 30 min at this temperature. All volatile materials were then removed in vacuo and the solid residue digested with pentane (200 mL). The salts were filtered through a reversed frit and washed with pentane (2×20 mL). The combined filtrates were reduced to dryness in vacuo and thoroughly dried thereafter. The deep yellow residue was of almost spectroscopic purity. Crystallisation from pentane (50 mL) at –30 °C yielded **1d** as yellow crystals. Yield: 8.17 g (75%) of bright-yellow **1d**, m.p. 134 °C (dec.). For spectroscopic data see ref.[6]

1-Methyl-2,4-bis(2′,3′,5′,6′-tetramethylphenyl)-3,5-bis(trimethylsilyl)-µ(1,2)-hydro-3-dehydro-1,2,4-triboracyclopentane (2a): A solution of freshly prepared **1a** (3.00 g, 6.17 mmol) in $CDCl_3$ (20 mL) was stored for 4 d at room temperature and the solution was monitored frequently by ^1H NMR spectroscopy. After completion of the reaction all volatile materials were removed in vacuo. The white residue consisted of essentially pure **2a** which could be crystallised at –30° from toluene. Yield: 2.97 g (99%) of white **2a**, m.p. 113 °C. ^1H NMR (500 MHz, $CDCl_3$, –40 °C): δ = 7.21, 6.99 (both s, 1 H each, Dur-H), 6.72 (br. s, 1 H, B–H–B), 2.49, 2.43, 2.37, 2.31, 2.28, 2.19 (all s, 24 H in total, Dur-CH_3), 1.10 (s, 1 H, CHSi), 0.66 (s, 3 H, BCH_3), 0.01, –0.26 (both s, 9 H each, $SiMe_3$) ppm. ^{13}C NMR (125 MHz, $CDCl_3$, –40 °C): δ = 146.7, 133.9 (each br. s, *i*-C), 140.0, 138.4, 134.0, 133.1, 133.05, 132.9, 132.8, 131.8 (each s, *o*- and *m*-C), 134.9, 129.6 (both d, *p*-C), 74.6 (s, B_2C), 27.6 [d, ^1J(C,H) = 116 Hz, B_2CH], 20.6, 20.5, 20.3, 20.1, 19.6, 19.3 (all q, Dur-CH_3), 4.9 [br. q, ^1J(C,H) = 117 Hz, BCH_3], 0.9, 0.2 (both q, $SiMe_3$) ppm. ^{11}B NMR (96 MHz, $CDCl_3$, 25 °C): δ = 56, 48, 0 (each 1B) ppm.

1-Phenyl-2,4-bis(2′,3′,5′,6′-tetramethylphenyl)-3,5-bis(trimethylsilyl)-µ(1,2)-hydro-3-dehydro-1,2,4-triboracyclopentane (2b): A solution of **1b** (5.67 g, 10.3 mmol) in $CDCl_3$ (25 mL) was stored for 9 d at room temperature and was monitored frequently by ^1H NMR spectroscopy. All volatile materials were then removed in vacuo and the residue was dissolved in a 1:1-mixture of Et_2O and pentane (30 mL). After four days at –30 °C **2b** precipitated as a white solid which was contaminated with approx. 5% of a product of unknown constitution. Yield: 1.97 g (35%) of white **2b**, m.p. 128 °C. ^1H NMR (500 MHz, $CDCl_3$, 25 °C): δ = 7.5 (br., BHB, located by $^1H/^1H$ COSY to d at 1.43), 7.5, 7.4 (br.s, 6 H in total, Ph–H and B–H–B), 7.17, 6.91 (both s, 1 H each, Dur-H), 2.61, 2.32, 2.28, 2.20, 2.2 (br.), 1.7 (br) (all s, 24 H in total, Dur-Me), 1.43 [d, ^3J(H,H) = 4.6 Hz, 1 H, CHSi, identified by a cross peak to $\delta^{13}C$ = 26.8 in a C,H correlated spectrum], 0.09, –0.12 (both s, 9 H each, $SiMe_3$) ppm. ^1H NMR (500 MHz, $CDCl_3$, –40 °C) 7.7–7.6 (br., 6 H in total, Ph–H and B–H–B), 7.24, 6.99 (both s, 1 H each, Dur-H), 2.65, 2.36, 2.31, 2.29, 2.28, 2.18, 2.02, 1.67 (all s, 3 H each, Dur-Me), 1.51 [d, ^3J(H,H) = 4.6 Hz, 1 H, CHSi], 0.09, –0.12 (both s, 9 H each, $SiMe_3$) ppm. ^{13}C NMR (75 MHz, $CDCl_3$, 25 °C): δ = 146.8 (br. s, *i*-C), 140.8, 139.8, 134.0, 133.5, 132.9, 132.5 (all s, Dur-*o*- and *m*-C), 136.7, 127.3 (both d, Ph-*o*- or *m*-C), 135.5, 130.0 (both d, Dur-*p*-C), 128.3 (d, Ph-*p*-C), 71.9 (br. s, B_2C), 26.8 [d, ^1J(C,H) = 113 Hz, B_2CH], 21.1, 20.3, 20.2, 20.0, 19.55, 19.50 (all q, Dur-CH_3), 1.6, 0.8 ppm (both q, $SiMe_3$), Ph-*i*-C and one Dur-*i*-C not observed. ^{13}C NMR (125 MHz, $CDCl_3$, –40 °C): δ = 146.5, 139.2 (both br., Dur-*i*-C′s), 141.0, 139.7, 133.9, 133.4, 133.0,. 132.9, 132.6, 132.3 (Dur-*o*- and *m*-C′s), 136.6, 127.2 (br., Ph-*o*- or *m*-C′s), 135.5, 129.7 (Dur-*p*-C′s), 133.1 (br., Ph-*i*-C), 128.2 (Ph-*p*-C), 70.7 (B_2C), 26.4 (B_2CH), 21.0, 20.6, 20.4, 20.3, 20.0, 19.9, 19.6, 19.5 (Dur-CH_3), 1.4, 0.6 ($SiMe_3$) ppm. ^{11}B NMR (160 MHz, $CDCl_3$, 25 °C): δ = 57, 42, –2 ppm (each 1B).

1,2,4-Tris(2′,3′,5′,6′-tetramethylphenyl)-3,5-bis(trimethylsilyl)-µ(1,2)-hydro-3-dehydro-1,2,4-triboracyclopentane (2c): A mixture of **1d** (5.5 g, 10.85 mmol) and lithium powder (0.25 g) in diethyl ether (70 mL) was stirred at room temperature and monitored frequently by ^{11}B NMR spectroscopy until the signals of **1d** were replaced by those of **3** at δ = 24 and 21 ppm (about 1 h). After cooling to –78 °C, duryllithium (1.53 g, 10.85 mmol) was added with stirring. Formation of the dianion of **1c** during warming to room temperature was indicated by the presence of a ^{11}B NMR signal at δ = –16 ppm. After disappearance of the signals of **3** and cooling to –78 °C, 2,3-dibromo-2,3-dimethylbutane (2.6 g, 10.85 mmol) was added and the mixture allowed to warm to room temperature with stirring for an additional 1 h. ^{11}B NMR signals at δ = 97 and 80 ppm unambiguously indicated the formation of **1c**. All volatile materials were removed in vacuo and the residue was dissolved in pentane (50 mL). The salts were separated by filtration with a reversed frit and washed further with pentane (10 mL). The filtrate was reduced to dryness in vacuo yielding yellow **2c** which could be crystallised at –30 °C from pentane**.** Yield: 6.2 g (84%) of yellow **2c**, m.p. 134 °C. ^1H NMR (500 MHz, CD_2Cl_2, 25 °C): δ = 7.87 (br., 1 H, BHB), 7.02, 6.98 (both s, 1H and 2 H, respectively, *p*-H), 2.30, 2.26, 2.20, 2.10, 1.95 (all s, 36 H in total, Dur-Me), 1.17 (d, ^1J = 6.2 Hz, 1 H, CHSi), 0.06, –0.15 (both s, 9 H each, $SiMe_3$) ppm. ^{13}C NMR (125 MHz, CD_2Cl_2, 25 °C): δ = 143.4 (br. s, *i*-C), 136.9, 133.9, 133.6, 133.4 (all s, Dur-*o*- and *m*-C), 132.6, 131.0 (all d, 1C and 2C, *p*-C), 102.3 (br. s, B_2C), 25.0 (br. B_2CH), 21.1, 19.9, 19.7, 19.6 (all q, Dur-CH_3), 1.6, 0.9 (both q, $SiMe_3$) ppm. ^{13}C NMR (125 MHz, CD_2Cl_2, –90 °C): δ = 149.0, 146.0, 142.3, 137.5, 136.0, 135.6, 135.0, 134.5, 133.3,. 132.5, 132.1, 131.6 (*o*- *m*- and *i*-C′s), 131.6, 130.1, 129.1 (*p*-C), 89.1 (B_2C), 21.6 (B_2CH), 22.2, 21.6, 21,4, 20.3, 20.2, 20.1, 19.1, 18.7, 18.1 (Dur-CH_3), –0.01, –0.21 ($SiMe_3$) ppm. ^{11}B NMR (96 MHz, $CDCl_3$, 25 °C): δ = ca. 47 (2B), ca. 30 ppm (1B).

X-ray Crystal Structure Analyses of 1a, 2a, 2b and 2c·pentane: Single crystals were grown from toluene/Et_2O at 0 °C for **2a** and pentane at –30 °C for **2b** and **2c**. Those of **1a** were obtained from diethyl ether at –30 °C. The crystals were investigated on imaging plate systems (IPDS Stoe) using graphite monochromated Mo-K_α radiation at 193 K. The space groups were determined from the

Table 3. Crystal and experimental data for the structure determinations of **1a**, **2a**, **2b** and **2c**·pentane.

	1a	**2a**	**2b**	**2c**·pentane
Empirical formula	$C_{29}H_{49}B_3Si_2$	$C_{29}H_{49}B_3Si_2$	$C_{34}H_{51}B_3Si_2$	$C_{43}H_{71}B_3Si_2$
Formula mass	486.29	486.29	548.36	676.61
Measuring temperature	193 K	193 K	193 K	193 K
Crystal system	monoclinic	triclinic	monoclinic	triclinic
Space group	$P2_1/c$	$P\bar{1}$	$P2_1/c$	$P\bar{1}$
Unit cell a [pm]	1187.1(1)	877.8(1)	2036.4(1)	15.985(2)
b [pm]	1427.7(1)	1131.1(2)	1121.6(1)	16.758(2)
c [pm]	1905.1(1)	1725.1(3)	1596.7(1)	17.223(2)
α [°]	90	96.37(1)	90	77.21(1)
β [°]	104.45(1)	97.65(1)	110.49(1)	79.31(2)
γ [°]	90	109.46(1)	90	89.87(2)
Volume [Å^3]	3126.7(4)	1578.3(4)	3416.2(4)	4417.5(9)
Z	4	2	4	4
Calculated density [g cm^{-3}]	1.033	1.023	1.066	1.017
Absorption coefficient [mm^{-1}]	0.128	0.127	0.124	0.107
$F(000)$	1064	532	1192	1488
crystal size [mm]	0.55 × 0.40 × 0.10	0.30 × 0.30 × 0.05	0.30 × 0.25 × 0.15	0.45 × 0.30 × 0.05
Θ_{max} [°]	25.02	24.97	25.98	25.96
Index range	–14/14, –16/16, –22/22	–10/10, –13/13, –20/20	–25/24, –13/13, –19/19	–19/19, –20/20, –21/21
Scan type	ω-scans	ω-scans	φ-scans	φ-scans
No. of reflections	23617	14411	23778	42952
Unique refl., (R_{int})	5467 (0.0399)	5408 (0.0905)	6647 (0.0624)	16051 (0.1418)
Observed refl. [$I > 2\sigma(I)$]	4529	2878	3669	4713
Parameters, data/param. ratio	331, 16.5	330, 16.4	374, 17.8	916, 17.5
Goodness-of-fit (F^2)	1.071	0.904	0.814	0.852
R [$I > 2\sigma(I)$]	0.0375	0.0588	0.0403	0.0771
wR_2 (all refl.)	0.1140	0.1572	0.0879	0.1829
Largest diff. peak/hole [e Å^{-3}]	+0.173/–0.214	+0.303/–0.234	+0.259/–0.212	+0.462/–0.259

systematic absences and intensity statistics, no absorption corrections were applied. The structures were solved by direct methods and refined against all F^2 data using full-matrix least-squares and difference Fourier techniques [SHELX programmes[10,11]]. Most hydrogen atoms were kept riding in calculated positions with isotropic displacement factors taken as 1.2 times (1.5 times for CH_3) the U_{eq} value of the corresponding C atom. The hydrogen atoms at the central ring were located and refined with individual isotropic displacement factors. For all heavier atoms, anisotropic displacement parameters were used. The structure of **2c**·pentane showed two independent molecules and, in addition, two strongly vibrating or disordered pentane molecules in the asymmetric unit. The solvent molecules were refined with restraints in geometry and in the anisotropy of the displacement factors. Due to this problem and the weak data set [29% of reflections $> 4\sigma(F)$ only] the precision of the structural data is reduced. Details of the experimental and crystal data are summarised in Table 3. Crystallographic data (excluding structure factors) for the structures reported in this paper have been deposited with the Cambridge Crystallographic Data Centre as supplementary publication no. CCDC-245202 (for **1a**), -245204 (for **2a**), -245203 (for **2b**) and -245205 (for **2c**). Copies of the data can be obtained free of charge on application to CCDC, 12 Union Road, Cambridge CB2 1EZ, UK [Fax: +44-1223-336-033; E-mail: deposit@ccdc.cam.ac.uk]

Acknowledgments

This work was supported by the Deutsche Forschungsgemeinschaft (SPP Polyeder) and the Fonds der Chemischen Industrie.

---

[1] K. Sorger, P. von Ragué Schleyer, *J. Mol. Struct. (Theochem.)* **1995**, *338*, 317–346 and literature cited therein.; S. Fau, G. Frenking, *J. Mol. Struct. (Theochem.)* **1995**, *338*, 117–130.

[2] D. Steiner, C. Balzereit, H.-J. Winkler, N. Stamatis, M. Hofmann, P. von Ragué Schleyer, W. Massa, A. Berndt, *Angew. Chem.* **1994**, *106*, 2391–2394; *Angew. Chem. Int. Ed. Engl.* **1994**, *33*, 2303–2306.

[3] M. Menzel, D. Steiner, H.-J. Winkler, D. Schweikart, S. Mehle, S. Fau, G. Frenking, W. Massa, A. Berndt, *Angew. Chem.* **1995**, *107*, 368–370; *Angew. Chem. Int. Ed. Engl.* **1995**, *34*, 327–329.

[4] A. Krämer, J.-K. Uhm, S. E. Garner, H. Pritzkow, W. Siebert, *Z. Naturforsch.* **1990**, *45b*, 1019–1021.

[5] a) G. E. Herberich, C. Ganter, L. Wesemann, *Chem. Ber.* **1990**, *123*, 49–51; b) G. Knörzer, H. Seyffer, W. Siebert, *Z. Naturforsch., Teil B* **1990**, *45*, 1136–1138.

[6] D. Scheschkewitz, A. Ghaffari, P. Amseis, M. Unverzagt, G. Subramanian, M. Hofmann, P. von Ragué Schleyer, H. F. Schaefer III, G. Geiseler, W. Massa, A. Berndt, *Angew. Chem.* **2000**, *112*, 1329–1332; *Angew. Chem. Int. Ed.* **2000**, *39*, 1272–1275.

[7] All structures were optimized at the MP2(fc)/6-311+G** level and relative energies were determined at the MP4SDTQ/6-311+G**//MP2(fc)/6-311+G** + 0.93 ZPE[MP2(fc)/6-311+G**] level using Gaussian 98: M. J. Frisch, G. W. Trucks, H. B. Schlegel, G. E. Scuseria, M. A. Robb, J. R. Cheeseman, V. G. Zakrzewski, J. A. Montgomery Jr., R. E. Stratmann, J. C. Burant, S. Dapprich, J. M. Millam, A. D. Daniels, K. N. Kudin, M. C. Strain, O. Farkas, J. Tomasi, V. Barone, M. Cossi, R. Cammi, B. Mennucci, C. Pomelli, C. Adamo, S. Clifford, J. Ochterski, G. A. Petersson, P. Y. Ayala, Q. Cui, K. Morokuma, D. K. Malick, A. D. Rabuck, K. Raghavachari, J. B. Foresman, J. Cioslowski, J. V. Ortiz, B. B. Stefanov, G. Liu, A. Liashenko,

P. Piskorz, I. Komaromi, R. Gomperts, R. L. Martin, D. J. Fox, T. Keith, M. A. Al-Laham, C. Y. Peng, A. Nanayakkara, C. Gonzalez, M. Challacombe, P. M. W. Gill, B. Johnson, W. Chen, M. W. Wong, J. L. Andres, C. Gonzalez, M. Head-Gordon, E. S. Replogle, J. A. Pople, *Gaussian 98*, Revision A.6, Gaussian, Inc., Pittsburgh PA, **1998**.

[8] M. Unverzagt, G. Subramanian, M. Hofmann, P. von Ragué Schleyer, S. Berger, K. Harms, G. Geiseler, W. Massa, A. Berndt, *Angew. Chem.* **1997**, *109*, 1567–1569; *Angew. Chem. Int. Ed. Engl. Ed.* **1997**, *36*, 1469–1472.

[9] At the MP2/6-31G* level nonclassical **VIu** is more stable than classical **III** by 2.5 kcal mol^{-1}: ref.[2].

[10] G. M. Sheldrick, *SHELXS-97, Program for the Solution of Crystal Structures*, University of Göttingen, **1997**.

[11] G. M. Sheldrick, *SHELXL-97, Program for the Refinement of Crystal Structures*, University of Göttingen, **1997**.

Received: March 31, 2005